Polymer Journal (2011) 43, 249–257

www.nature.com/pj

ORIGINAL ARTICLE

Complementary functionality of SiO_2 and TiO_2 in polyimide/silica–titania ternary hybrid nanocomposites

Wen-Chang Liaw[1], Yu-Lin Cheng[1], Yu-Sun Liao[2], Chee-Shan Chen[3] and Shih-Ming Lai[1]

A polyimide (PI) composite containing SiO_2 and TiO_2 hybridized nanoparticles was prepared by the sol-gel process. Polyamic acid (PAA) solution, the precursor of PI, was synthesized from 2,2′-bis-(3,4-dicarboxyphenyl) hexofluoropropane dianhydride and bis [4-(3-aminophenoxy) phenyl sulfone in *N*-methyl-2-pyrrolidone. The SiO_2–TiO_2 hybrid nanoparticles were prepared by the sol-gel process in a PAA solution into which tetraethoxysilane, titanium (IV) tetrabutoxide and acetylacetone were mixed for subsequent hydrolysis and condensation reactions. After spin coating of this solution onto a glass substrate, the stepwise imidization to PI and the simultaneous gelation of the SiO_2–TiO_2 hybrid oxides were achieved at 100–300 °C. The complementing effects of reduced particle size and enhanced thermal stability of SiO_2 and TiO_2 on the resulting nanocomposite were observed. The former effect was contributed by TiO_2 and the latter by SiO_2. Uniform dispersion of 5- to 10-nm-diameter SiO_2–TiO_2 nanoparticles was obtained in the PI matrix. A 5-μm-thick film obtained from this procedure exhibited excellent optical transparency (91%, 500 nm) at 15 wt% SiO_2 for a TiO_2 content <5 wt%.
Polymer Journal (2011) **43,** 249–257; doi:10.1038/pj.2010.117; published online 19 January 2011

Keywords: calcination; morphology; polyimide; ternary hybrid nanocomposites

INTRODUCTION

Organic–inorganic composite materials combine the advantages of both classes while simultaneously providing more design variables. Quite often, however, certain technical difficulties need to be overcome because of the presence of two distinct organic–inorganic phases. Control over particle size and interface compatibilization are two such major issues of concern.

In general, the smaller the size of the inorganic particle, the larger is its available surface area for enhancing the reinforcement of the continuous organic phase while simultaneously improving macroscopic homogeneity and optical properties. Recent advancements in nanotechnology have opened a new era in the synthesis of organic–inorganic hybrid nanocomposites, with nanosized inorganic particles that may provide a new category of materials with desirable characteristics in various applications.[1–3]

Polyimides (PI) are important, high-performance polymer materials characterized by their superior thermal stability and mechanical strength. They have been widely used in microelectronic and aerospace applications. The mechanical and thermal properties of PI polymers can be further enhanced or tailored to meet widely varied demands by combining them with various inorganic metal oxides by *in situ* polymerization and sol-gel processes. These processes have been adapted to the preparation of organic–inorganic hybrid nanocomposites. It has been shown that the morphology of the resulting metal oxides in the composite may be improved by tuning the formulation and processing conditions.

Some researchers have studied the preparation and properties of the binary hybrid nanocomposites PI/SiO_2[4–10] and PI/TiO_2.[11–17] In our previous papers,[18,19] we reported on the preparation of binary hybrid films of poly(imide siloxane) (PIS)/SiO_2 and PIS/TiO_2. In synthesizing the PIS/silica (SiO_2) hybrid nanocomposite, a C–Si covalent bond was formed between the homogeneous PIS copolymer and SiO_2 with the aid of a silicon coupling agent.[18] This C–Si covalent bond was found to successfully enhance the dispersion of the inorganic SiO_2 in the organic phase and reduce the particle size to <60 nm (SiO_2 content <10 wt%). Consequently, the material's mechanical and thermal properties were significantly improved.[18]

Using a similar method applied to the preparation of PIS/titania (TiO_2) hybrid nanocomposites, TiO_2 was well dispersed in a PIS matrix by the sol-gel process to keep the particle size below 50 nm (TiO_2 content <20 wt%). The nanocomposite exhibited good optical transparency whereas the mechanical and thermal properties were only slightly compromised.[19]

Another category of PI–metal oxide hybrid composites is the ternary hybrids of PI/SiO_2–TiO_2, which are expected to possess good thermal stability (due to SiO_2), small particle size and an adjustable refractive index (due to TiO_2). However, there are few reports that discuss these types of hybrid nanocomposites. Wang *et al.*[20] prepared PI/SiO_2–TiO_2 hybrid films through a non-hydrolytic sol-gel route from silicic acid and titanium tetrachloride. They reported that the optical properties of the hybrid films exhibited a red shift of the absorption band that increased with increasing

[1]Department of Chemical and Materials Engineering, National Yunlin University of Science and Technology, Yunlin, Taiwan; [2]Department of Materials Science and Engineering, Feng Chia University, Taichung, Taiwan and [3]Department of Applied Chemistry, Chaoyang University of Technology, Taichung County, Taiwan
Correspondence: Professor W-C Liaw, Department of Chemical and Materials Engineering, National Yunlin University of Science and Technology, #123, Section 3, University Road, Touliu, Yunlin 64002, Taiwan.
E-mail: liawwc@yuntech.edu.tw
Received 1 June 2010; revised 29 September 2010; accepted 8 October 2010; published online 19 January 2011

TiO_2 content, whereas all hybrid films maintained good transparency. The thermal decomposition temperature of the ternary hybrid films decreased slightly with increasing TiO_2 content. Qiu *et al.*[21] prepared ternary hybrid PI/SiO_2–TiO_2 films with SiO_2 to TiO_2 ratios of 1:2, 1:1 and 2:1 and found that such ternary hybrids exhibited desirable optical properties without significantly sacrificing physical and thermal properties.

In general, the well-known role of SiO_2 in PI-composite materials is the enhancement of thermal and mechanical properties. On the other hand, incorporating TiO_2 is known for its functionality in particle size control and optical property modulation. However, because of its photocatalytic character, the presence of TiO_2 tends to decrease the thermal stability of the material. It is quite likely that combining the two would complement each other, thus widening the range of design variables, as has been shown in literature.[20,21] However, 'complementing' normally leads to 'compromising,' and the manner in which the degree of compromise is controlled within a tolerable range is important in the design of composite materials of this kind.

This study takes a systematic approach to understanding the ternary PI/SiO_2–TiO_2 nanocomposite. Major issues concerning industrial applications, such as the manner in which the SiO_2–TiO_2 ratio affects the thermal degradation temperature (T_d), inorganic particle size and mechanical properties, will be discussed and compared. At the same time, studying the formation of the Si–O–Ti bond will help explain the complementing role of Si and Ti in the nanocomposites.

In the sol-gel process, the gelation of TiO_2 occurs rapidly.[22,23] Consequently, TiO_2 will form aggregates before having a chance to react with neighboring SiO_2 in the ternary system. The rapid gelation rate of titanium alkoxide to TiO_2 has been observed for the binary PI/TiO_2,[22] which will inevitably generate an undesirable morphology of the obtained TiO_2. Complex formation of the titanium ion with certain ligands or chelating agents may be an option to stabilize the titanium ion and circumvent this problem.[22–24] Specifically because acetylacetone (acac) is capable of chelating with transition metals,[13,15,16] it was introduced to partially offset the fast gelation rate of titanium to manipulate the resulting morphology and physical properties of the composite.

EXPERIMENTAL PROCEDURE

Materials

Diamine, bis [4-(3-aminophenoxy) phenyl] sulfone (m-BAPS, 97%), was purchased from Tokyo Kasei Kogyo Co., Ltd (Tokyo, Japan). Dianhydride, 2, 2′-bis-(3, 4-dicarboxyphenyl) hexafluoropropane dianhydride (6FDA, 99%), was purchased from Chriskev Co., Ltd (Lenexa, KS, USA). *N*-methyl-2-pyrrolidone (NMP, 99%) was purchased from Mallinckrodt Chemicals Inc. (Phillipsburg, NJ, USA; http://www.mallbaker.com/americas/msds/english/M7114_msds_us_cov_Default.pdf) and dried with 4 Å molecular sieves. Tetraethoxysilane (TEOS, 99%) was purchased from Fluka Chemical Corp. (St Louis, MO, USA; http://www.sigmaaldrich.com/catalog/ProductDetail.do?D7=0&N5=Product%20No.%7CBRAND_KEY&N4=86580%7CFLUKA&N25=0&QS=ON&F=SPEC). Titanium (IV) tetrabutoxide (TBT, 99%) was purchased from Acros Organics (Geel, Belgium). Acetylacetone (99%) was purchased from Merck (Darmstadt, Germany).

In designing the organic matrix for the composite, reference was made to a report by Ando[25] stating that, among its many attractive attributes, fluorinated polyimide exhibits improved optical transparency compared with conventional PI. Therefore, 6FDA was chosen for this study. It was also mentioned in his report that the participation of sulfon (–SO_2–) linkage would blue shift the absorption edges for PIs derived from 6FDA.

Liaw and Liaw[26] used polymers aryl sulfone linages, bis [4-(4-aminophenoxy) phenyl] sulfone (BAPS), in synthesizing BAPS-derived PI. According to their report, BAPS has a number of advantages, including its amorphous character, low glass transition temperature, high thermo-oxidative stability and excellent mechanical properties. For similar reasons, m-BAPS was chosen for the synthesis of PI in this study.

Preparation of silica precursor

The silica precursor solution was prepared by mixing 1 mol of TEOS with 4 mol of distilled water. A small quantity of NMP was then added to the solution under a nitrogen atmosphere. The mixture was then vigorously agitated until it was homogeneous and transparent.

Preparation of titanium precursor

The titanium precursor solution was prepared by mixing 1 mol of TBT with 4 mol of acac under a nitrogen atmosphere. The mixture was then vigorously agitated until a homogeneous and transparent solution was obtained.

Preparation of PI/SiO_2–TiO_2 ternary hybrid nanocomposites

The polyamic acid (PAA) solution, the intermediate of PI polymerization, was prepared by the polycondensation of 6FDA with m-BAPS in NMP solution for 12 h at room temperature. Then, an appropriate amount of silica precursor was introduced into the prepared PAA solution and stirred. After the solution became clear (about 2 h), the titanium precursor solution was added, and the mixture was stirred again at room temperature for about 6 h until transparent. The PI/SiO_2–TiO_2 ternary hybrid nanocomposite films were prepared by casting the above mixture on a glass substrate, followed by stepwise imidization at 80, 100, 150, 200, 250 and 300°C for 1 h at each temperature.

Calcination of PI/SiO_2–TiO_2 nanocomposites

In a scanning electron microscopy (SEM) micrograph of the PI/SiO_2–TiO_2 ternary hybrid nanocomposite, the organic PI polymer would very likely block imaging of a significant portion of the inorganic particles. To obtain a clear view of the inorganic SiO_2–TiO_2 particles in PI/SiO_2–TiO_2 hybrid nanocomposites, calcination of the prepared hybrid nanocomposites was conducted at 600°C for 2 h to remove the organic portion (PI) of the hybrid nanocomposite. After calcination, the organic PI matrix is totally decomposed, and it is easier to observe the morphologies, particle size and geological distributions of the inorganic particles.

Characterization

The molecular weight of PAA was measured by gel permeation chromatography (RI-930 detector, Jasco, Tokyo, Japan) at room temperature. The PAA concentration was 1.25% w/v, and NMP was used as the eluent at a flow rate of 1 ml min^{-1}. Polystyrene was used as the standard. The inherent viscosity of PAA in NMP was also measured with an Ubbelohde viscometer at 30 °C.

Fourier transform infrared (FT-IR) spectra were recorded on a PerkinElmer Spectrum One FT-IR spectrometer (Shelton, CT, USA; http://las.perkinelmer.com/Content/RelatedMaterials/SpecificationSheets/spc_spectrumoneftir.pdf). Microscopic images of the fracture surface of PI/SiO_2–TiO_2 films were taken by a Scanning Electron Microscope (JEOL JSM-6701F, Japan). The chemical compositions of PI/SiO_2–TiO_2 films were analyzed by using X-ray photoelectron spectroscopy (ULVAC-PHI 5000, Japan). A transmission electron microscope (TEM) was used to observe the SiO_2–TiO_2 hybrid nanoparticles (JEOL JEM-200CX, Japan). Atomic force microscopy images were taken with a Scanning Probe Microscope (Veeco CP-II, USA). Thermal degradation and thermal stability of the films were monitored by a Thermogravimetric analysis (TA-Instruments 2050, USA). Thermalgravimetric analysis measurements were taken under a nitrogen atmosphere at a heating rate of 20 °C min^{-1} from 25 to 900 °C. Transparencies were measured on a UV–visible spectrometer (PerkinElmer UV/VIS/NIR lambda 850, PerkinElmer).

RESULTS AND DISCUSSION

This study mainly focused on the complementary effects of SiO_2 and TiO_2 on PI/SiO_2–TiO_2 ternary systems. As stated above, incorporating SiO_2 would improve the physical properties of the composite material. Incorporating TiO_2, on the other hand, would improve the material's optical refractive index with an inherent impact on the stability of the PI matrix.

According to our previous studies, SiO_2 affects the morphology of the PI/SiO_2 binary systems in such a manner that high SiO_2 content would result in large inorganic particles (2 μm at 15 wt%, Figures 5a and A). In contrast, TiO_2 forms small inorganic particles (5–10 nm at 15 wt%, Figures 5b and B). On the basis of our previous observations on binary systems and the expected complementation between the effects of SiO_2 and TiO_2 on the ternary system, we decided to fix the SiO_2 content at 15 wt% and adjust the TiO_2 content within 0–15 wt%.

In this study, the PI matrix was synthesized according to literature.[16] The molecular weight was fixed at about 100 000 Dalton (100 kDa). The *M*n, *M*w and molecular weight distribution of the PAA intermediate in this study were found to be 96 934, 109 315 and 1.13, respectively. The inherent viscosity at 0.5 g per 100 ml was 71 ml g^{-1} at 30 °C.

The mechanism of inorganic nanoparticle formation involves a two-step reaction. The first step is the hydrolysis of the inorganic alkoxides TEOS or TBT to form hydroxyl silicate or titanate. The hydrolysis intermediates then react with each other through a condensation reaction to form a three-dimensional inorganic network. When a chelating agent such as acac is added, $[Ti(acac)3]^+$ forms during a reaction between TBT and acetylacetone,[27] and the Ti–acac complex then slowly transforms into a gel-like product after the addition of water. This Ti–acac complex formation is important in forming Si–O–Ti bonds, as will be discussed below.

FT-IR spectra

During synthesis of the PI matrix, the intermediate was the PAA. Figure 1 shows the FT-IR absorption spectra of PAA (a), PI (b), PI/SiO_2 (c) and PI/TiO_2 (d). In Figure 1b, the absorption bands at 1780, 1730 and 720 cm^{-1} are characteristic of the imide group. Meanwhile, the disappearance of the absorption peak in Figure 1a corresponding to the amide function group at 1650 cm^{-1} indicates virtually complete imidization of PAA to PI, which is also supported by the flatness of the absorption band near 3600 cm^{-1} (−OH stretch, Figure 1b).

Figure 1c depicts the absorption peaks attributed to the formation of the Si–O–Si bond in the PI/SiO_2 composite, which was first derived from TEOS by the hydrolysis of Si–O–C_2H_5 to Si–OH and then subjected to a condensation reaction to form the Si–O–Si bonds.[4,5,7,9] The SiO_2 characteristic absorption band can be seen in the range of 1025–1100 cm^{-1} as broadened peaks when compared with PI (Figure 1b). Similarly, the characteristic absorption peaks of PI/TiO_2 (Figure 1d), corresponding to the Ti–O–Ti bond derived from the titanium precursor, were in the range of 450–850 cm^{-1}. This feature was observed as an upward-shifted baseline because of the broad TiO_2 absorption peak.[13–17] The absorption patterns of the transparent PI/SiO_2 and PI/TiO_2 films were quite similar to that of neat PI in other wavenumber ranges.

Figures 1e–i compare the FT-IR spectra of PI/SiO_2–TiO_2 (PI/S–T) composites of various compositions at a fixed SiO_2 content of 15 wt%. The TiO_2 content was changed from 2 to 15 wt%. Three important features of Figure 1 are discussed below.

SiO_2 absorption. In Figure 1c, the absorption peaks at 1100 and 1145 cm^{-1} are of similar height as those in neat PI. However, at 15 wt% SiO_2 (Figure 1c), the peak at 1100 cm^{-1} was apparently higher than at 1145 cm^{-1}, whereas the increase in absorption intensity at 1100 cm^{-1} extended to 1025 cm^{-1}. However, this PI/SiO_2 twin peak characteristic changed after TiO_2 was introduced into the composite. In Figures 1e–i, when the TiO_2 content was increased from 2 to 15 wt%, the 1000–1100 cm^{-1} band diminished accordingly. This leads to the speculation that, in the current case, Ti might have also participated in the formation of Si–O–Ti bonds in addition to Si–O–Si bonding.

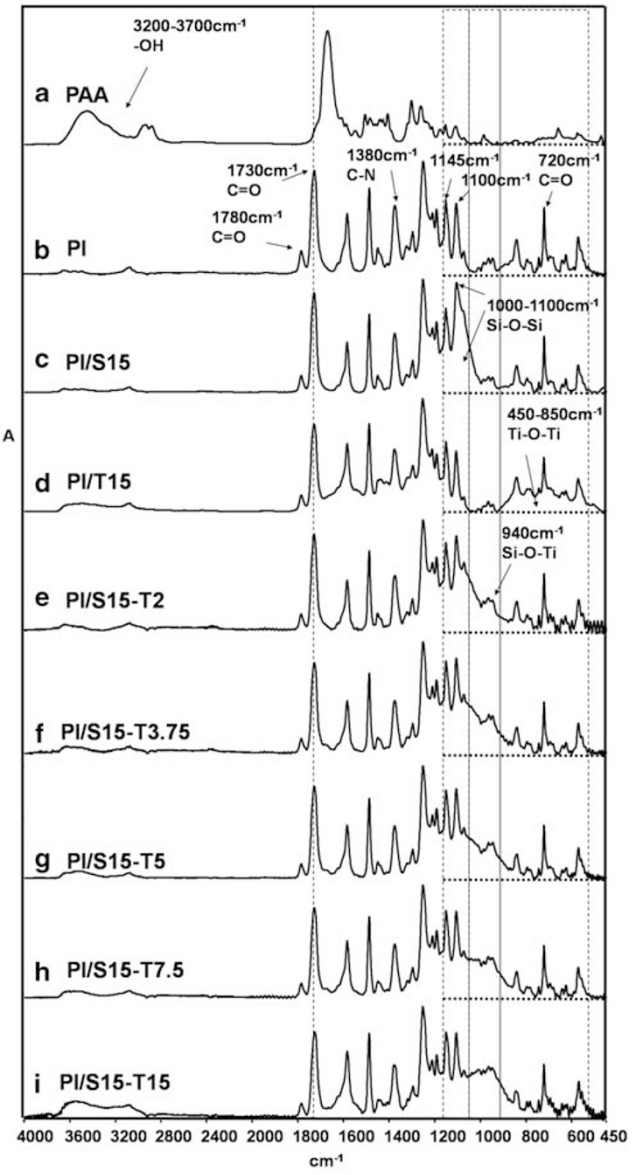

Figure 1 Fourier transform infrared spectra of (**a**) PAA, (**b**) PI, (**c**) PI/S15, (**d**) PI/T15, (**e**) PI/S15–T2, (**f**) PI/S15–T3.75, (**g**) PI/S15–T5, (**h**) PI/S15–T7.5 and (**i**) PI/S15–T15 hybrid nanocomposites. PAA, polyamic acid; PI, polyimide.

TiO_2 absorption. In the 450–850 cm^{-1} range shown in Figure 1d, the presence of TiO_2 was supposed to shift the baseline upward. However, in the presence of SiO_2 (15 wt%), depicted in Figures 1e–i, the increased TiO_2 content did not show a significant effect on the absorption pattern in this range. Rather, such a variation was reflected elsewhere (1025–850 cm^{-1}). This phenomenon suggests that the Ti–O–Ti bonds presented in the PI/TiO_2 system (Figure 1d) existed in the PI/SiO_2–TiO_2 system in a form other than the Ti–O–Ti bonds. Considering what has happened to the Si–O–Si bonding (broadening, Figure 1c), these variations further suggest that the Ti–O–Ti bonding might have shifted to the Si–O–Ti bonds on addition of TiO_2.

Si–O–Ti absorption. Figures 1c and d show the FT-IR spectra of the binary hybrids of the PI composite. In contrast to the spectrum of neat PI depicted in Figures 1e–i, the absorption pattern in the range of

1025–850 cm^{-1} varied with increasing TiO_2 content. This variation was observed as an upward shift of the baseline and was accompanied by a decrease in the baseline in the range of 450–850 cm^{-1} (Ti–O–Ti, in the PI/TiO_2 system). As stated above, this indicates that the TiO_2 added to the PI/SiO_2 system likely participates in bonds other than Ti–O–Ti. Qiu *et al.*[21] reported a similar observation, but this study provides more detailed information.

In summary, the changing patterns in the FT-IR spectra of SiO_2 absorption in the PI/SiO_2 composite, TiO_2 absorption in the PI/TiO_2 composite and the PI/SiO_2–TiO_2 composite revealed that a significant portion of Si–O–Si and Ti–O–Ti bonding had transformed to Si–O–Ti bonding in the PI/SiO_2–TiO_2 composite. This is an important route through which the two inorganic elements provide complementary effects on the composite.

The formation of Si–O–Ti bonds suggests that introducing 'acac' stabilized and retarded the fast gelation rate of TiO_2, providing opportunities for Si–O–Ti bond formation. Therefore, the chelating agent may have contributed to slowing the gelation rate of TiO_2 to match the slow reaction rate of SiO_2. The Si–O–Ti bond is an important feature in ternary systems and will be discussed in greater detail below.

The weak and broad absorption in the 3200–3700 cm^{-1} range was attributed to the −OH residue belonging to the uncondensed Si–OH and Ti–OH formed during the hydrolysis of the TEOS and TBT alkoxy groups.[7,13,14,16,17] Although the absorption was weak, its intensity increased with increasing TiO_2 content. At high TiO_2 content, the radii of the inorganic particles were small (Table 1), leading to increased specific surface areas. The uncondensed surface Si–OH and/or Ti–OH would be more visible in FT-IR spectra in this range, as shown in Figure 1. These surface –OH groups would theoretically form hydrogen bonds with the C=O groups of the PI matrix. This hydrogen bonding would cause the absorption peaks of the C=O to shift to a lower wavenumber. In Figure 1, the C=O peak shifted from 1730 cm^{-1} (for PI/S15) to 1723 cm^{-1} (for PI/S15–T15). Wu *et al.* reported a similar observation in their study of the PI/SiO_2 binary system.[28]

Discussion of these −OH residues and whether they are in the form of Si–OH or Ti–OH on the surfaces of the inorganic nano particles is beyond the scope of this report, but it may be an important perspective in explaining the phenomena observed in this study. This question will be investigated in our future research. However, these hydrogen bonds between the uncondensed –OH of the inorganic nanoparticles and the C=O group of the PI matrix are beneficial in compatibilizing the inorganic phase and the organic phase.

Table 1 Physical, thermal and optical properties of the hybrid nanocomposites

Sample code	*SiO_2 (wt%)*	*TiO_2 (wt%)*	*Particle size (nm)*	*Average roughness Ra (nm)*	*T_d (°C)*	*Transmittance 500 nm (%)*
PI	0	0	—	1.02	532	97
PI/S15	15	0	1500–2000	—	553	93
PI/T15	0	15	5–10	—	482	58
PI/S15–T2	15	2	300–400	4.99	541	92
PI/S15–T3.75	15	3.75	10–20	0.68	522	92
PI/S15–T5	15	5	5–10	0.55	513	91
PI/S15–T7.5	15	7.5	5–10	0.38	502	89
PI/S15–T15	15	15	5–10	0.35	499	73

Abbreviation: PI, polyimide.

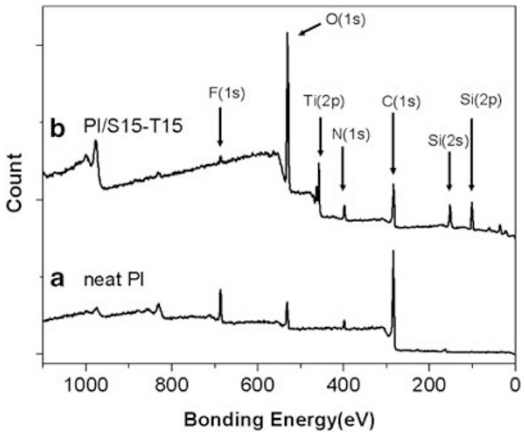

Figure 2 Full range of X-ray photoelectron spectra for the film surfaces of (**a**) polyimide (PI) and (**b**) PI/S15–T15 hybrid nanocomposites.

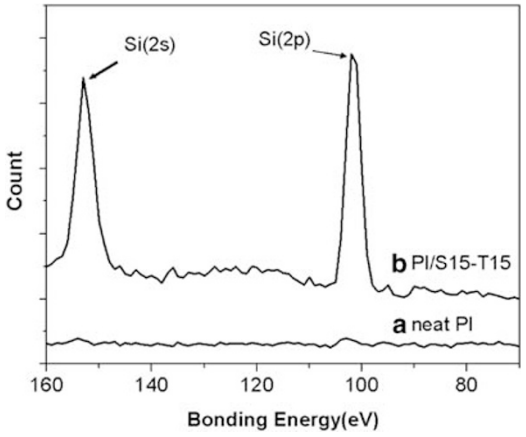

Figure 3 X-ray photoelectron spectra of Si(2s) and Si(2p) in (**a**) polyimide (PI) and (**b**) PI/S15–T15 hybrid nanocomposites.

X-ray spectra

X-ray photoelectron spectroscopy is a useful tool for providing information on the formation of chemical bonds between titanium and silicon atoms with other atoms (for example, oxygen, carbon and so on).[16] Figure 2 shows a typical wide-scan spectrum of the PI and PI/S15–T15 films produced in this study (SiO_2 content of 15 wt% and TiO_2 content of 15 wt%). In these spectra, the peaks due to C(1s), O(1s), N(1s), S(2p), F(1s), Si(2p) and Ti(2p) were detected at 295–280, 540–525, 410–395, 175–160, 684–690, 110–95 and 450–460 eV, respectively, consistent with the cited literature. This demonstrated the presence of elemental Si and Ti in the composites.

To extract more information from X-ray photoelectron spectroscopy, the spectrum in the region corresponding to Si(2p) and Ti(2p) was enlarged in Figures 3 and 4. Figure 3 shows two photoelectron peaks at 103.6 and 153 eV that reveal the presence of bulk Si(2p) and Si(2s), respectively.[29–32] Figure 4 shows two typical photoelectron peaks at 458 and 463 eV. These two peaks arise from bulk Ti(2p3/2) and surface Ti(2p1/2), respectively.[16,22,33] The relative intensities of these two peaks indicate that the amount of bulk Ti(2p3/2) (458 eV) is greater than that of surface Ti(2p1/2) (463 eV) because, at a fixed total amount of TiO_2, the bulk Ti peak was much higher than the surface Ti peak.

More bulk Ti indicates that the amount of surface Ti in direct contact with the PI matrix was reduced. Reduced surface titanium would alleviate its oxidative impact on the PI matrix and increase the thermal stability of the composites, as discussed in later sections.

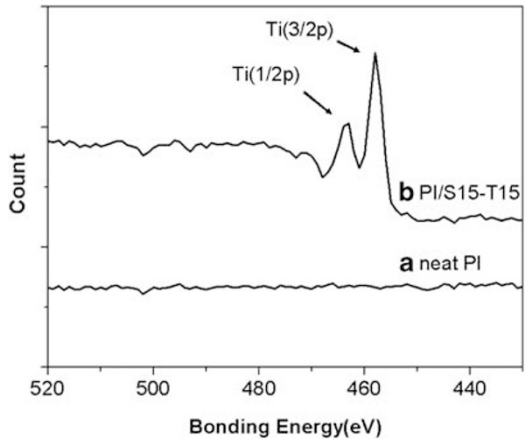

Figure 4 X-ray photoelectron spectra of Ti(2p) in (**a**) polyimide (PI) and (**b**) PI/S15–T15 hybrid nanocomposites.

More bulk Ti also indicates that most of the Ti participated in Si–O–Ti bonding. If this were not the case, distinct, small TiO_2 particles and relatively large SiO_2 particles would have been observed in the SEM and TEM micrographs discussed in the following sections. Furthermore, diminished Ti–O–Ti and Si–O–Si absorptions would not have been observed in the FT-IR spectra.

Morphology by SEM images

Figure 5 compares SEM micrographs of hybrid films of varying SiO_2 and TiO_2 content. Figure 5 is arranged into two sets: 5a–5h (SEM micrographs of the fracture surface of the composite films) and 5A–5H (SEM micrographs of the composite films after calcination). These micrographs show that, without calcination, most of the inorganic particles were buried in the organic matrix; only those exposed inorganic particles on the fracture surface were observable. Removing the organic moiety to expose the inorganic particles by calcination provided a better view of the size distribution and shape of the inorganic particles, as shown in Figure 5.

The composite films were subjected to calcination (at 600 °C, 2 h) for SEM micrograph, as shown in Figures 5A–H. These micrographs show that a better view of the inorganic particles is obtained after calcination. The size distribution and shape of the inorganic particles were rather uniform (Figures 5A–H). Wang *et al.*[20] and Qiu *et al.*[21] provided SEM micrographs of the composite without calcination.

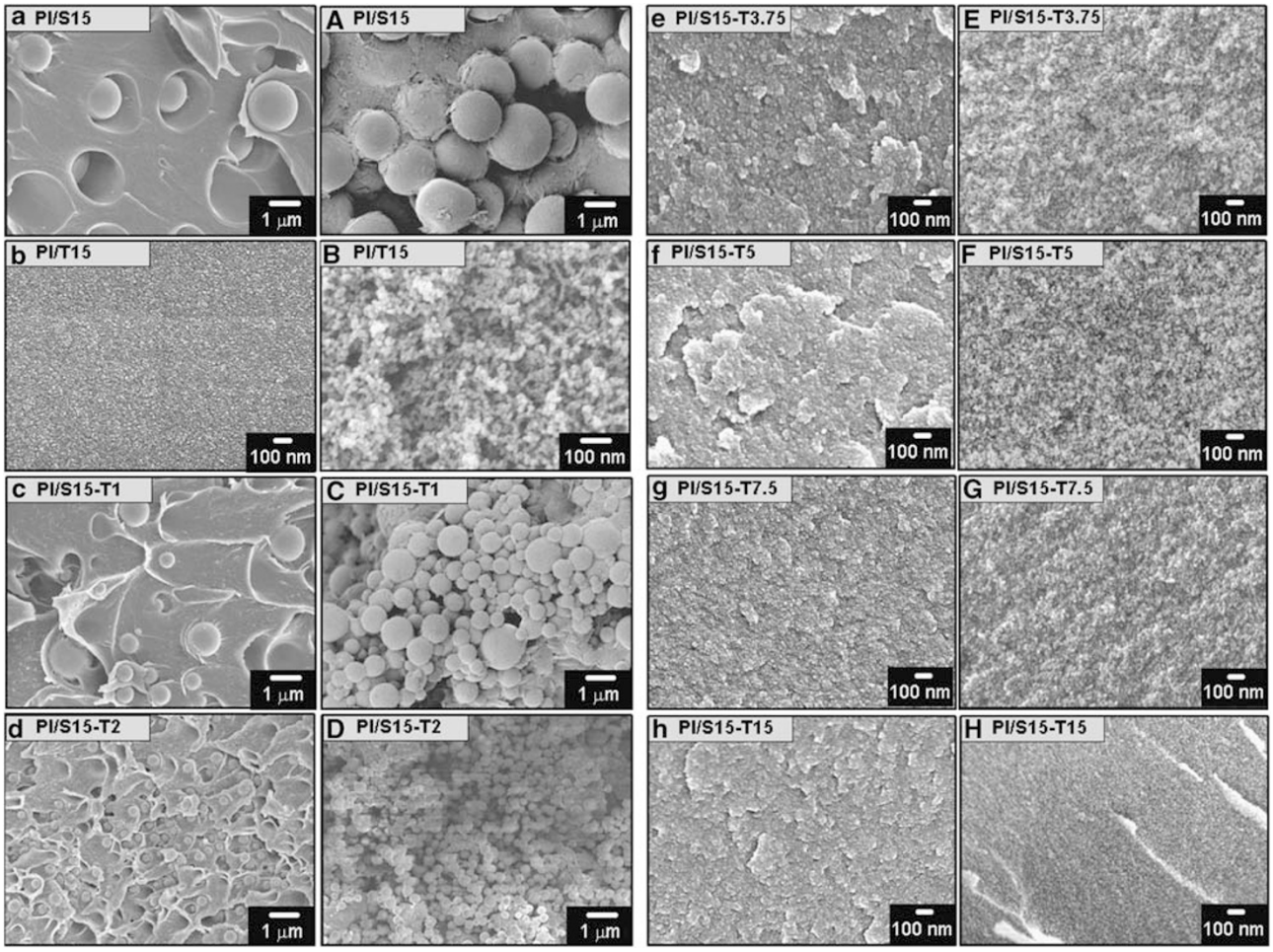

Figure 5 Comparison of scanning electron microscopy images of the polyimide (PI)/SiO_2–TiO_2 hybrid composites before ((**a**)–(**h**)) and after ((**A**)–(**H**)) calcination.

In the PI/SiO_2 and PI/TiO_2 binary systems, the SiO_2 particles were relatively large (1500–2000 nm, Figure 5A, Table 1) as compared with the TiO_2 particles (5–10 nm, Figure 5b, Table 1). According to this, in the ternary systems, if TiO_2 was not hybridized with SiO_2, discrete small TiO_2 particles would have been observed as inorganic particles much smaller than average in the calcinated PI/S15–T1, PI/S15–T2 and PI/S15–T3.75 (Figures 5C–5E). The inorganic particles decreased in size to 5–20 nm at a titanium content higher than 3.75 wt%, as shown in Table 1. This indicates that most of the TiO_2 was hybridized with SiO_2. This observation echoes the observation derived from the FT-IR data that a significant amount of Si–O–Ti bonds were formed, causing the Ti–O–Ti and Si–O–Si peaks to diminish in the ternary systems. Such a judgment would be difficult to make in SEM micrographs without calcination because the small TiO_2 particles, if not hybridized, would most likely be buried in or blocked by the PI matrix.

Another important feature exhibited in Figure 5 is that, unlike the morphology of binary systems, in the ternary hybrid films, the inorganic particles were much more homogeneously distributed and were presented as finely interconnected domains.

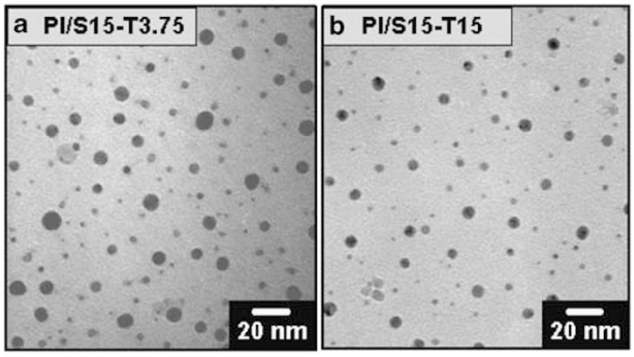

Figure 6 Transmission electron microscopy images of polyimide (PI)/SiO_2–TiO_2 ternary hybrid nanocomposites, (**a**) PI/S15–T3.75, (**b**) PI/S15–T15.

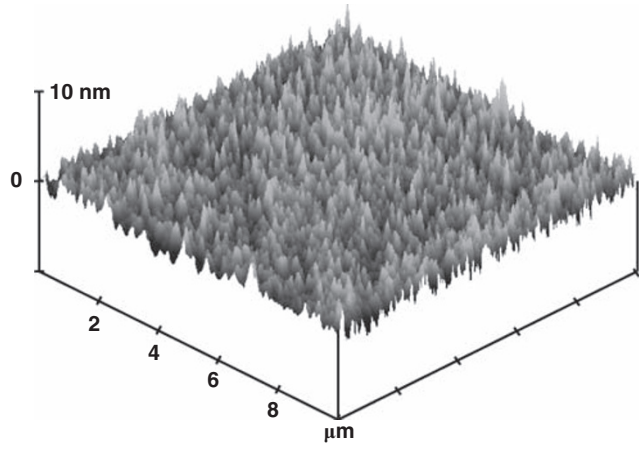

Figure 7 Atomic force microscopy diagram of the polyimide (PI)/SiO_2–TiO_2 ternary hybrid nanocomposites (PI/S15–T3.75).

Morphology of TEM images

When the TiO_2 content was >3.75 wt% in the ternary system, the inorganic particle size decreased to <20 nm (Figure 5E). TEM is a better tool than SEM to determine particle morphology. Figure 6 illustrates TEM micrographs for TiO_2 contents of (a) 3.75 and (b) 15 wt% when the SiO_2 content was fixed at 15 wt%. The typical size of the inorganic particles ranged from 4 to 8 nm. Comparing the two micrographs in Figure 6, we note that when the TiO_2 content was increased from 3.75 to 15 wt% no further reduction in the particle size was observed. This is consistent with our previous observations on TiO_2 in binary systems.[19] The micrographs in Figure 6 show that the size and shape of the inorganic particles were rather uniform. Large SiO_2 particles were not observed, indicating that the material is macroscopically homogeneous. This is consistent with the results stated above on both the postcalcinated SEM micrographs and the diminished Si–O–Si peak in the FT-IR spectra.

Morphology of AFM images

Figure 7 shows atomic force microscopy images of the surfaces of the PI/SiO_2–TiO_2 ternary hybrid nanocomposite films with

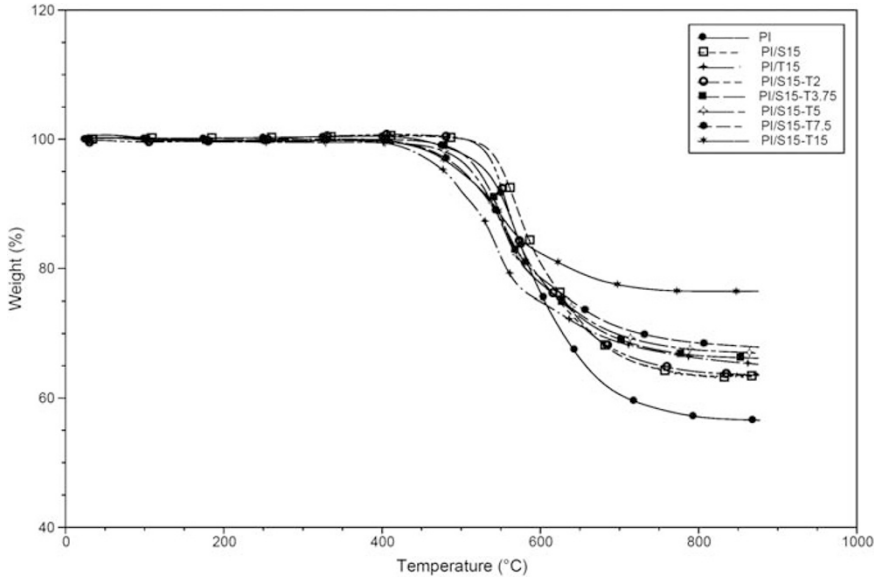

Figure 8 Thermal-gravimetric analysis curves of the polyimide (PI)/SiO_2–TiO_2 hybrid nanocomposites.

15 wt% SiO_2 and 3.75 wt% TiO_2. The measured average roughness (*R*a) of the neat PI polymer film was 1.02 nm (Table 1). When inorganic SiO_2 (15 wt%) and TiO_2 (2 wt%) were incorporated, the inorganic particle size was ~300–400 nm, increasing the *R*a to 4.99 nm. However, because of the aforementioned functionality of TiO_2 in particle size control, when TiO_2 was further increased to 3.75, 7.5 and 15 wt%, the *R*a decreased to 0.68, 0.38 and 0.35, respectively (Table 1).

Comparing the above values of *R*a with those of the neat PI and PI/S15–T2 systems, the increased TiO_2 was apparently reflected in the reduced roughness. However, the magnitude of *R*a was far smaller than the diameters of the inorganic SiO_2–TiO_2 particles (0.35–0.68 nm compared with 5–10 nm, Table 1). This suggests that at appropriate concentrations TiO_2 contributes to reducing the inorganic particle size and improving homogeneity, consequently reducing the surface roughness of the ternary hybrid composite system.

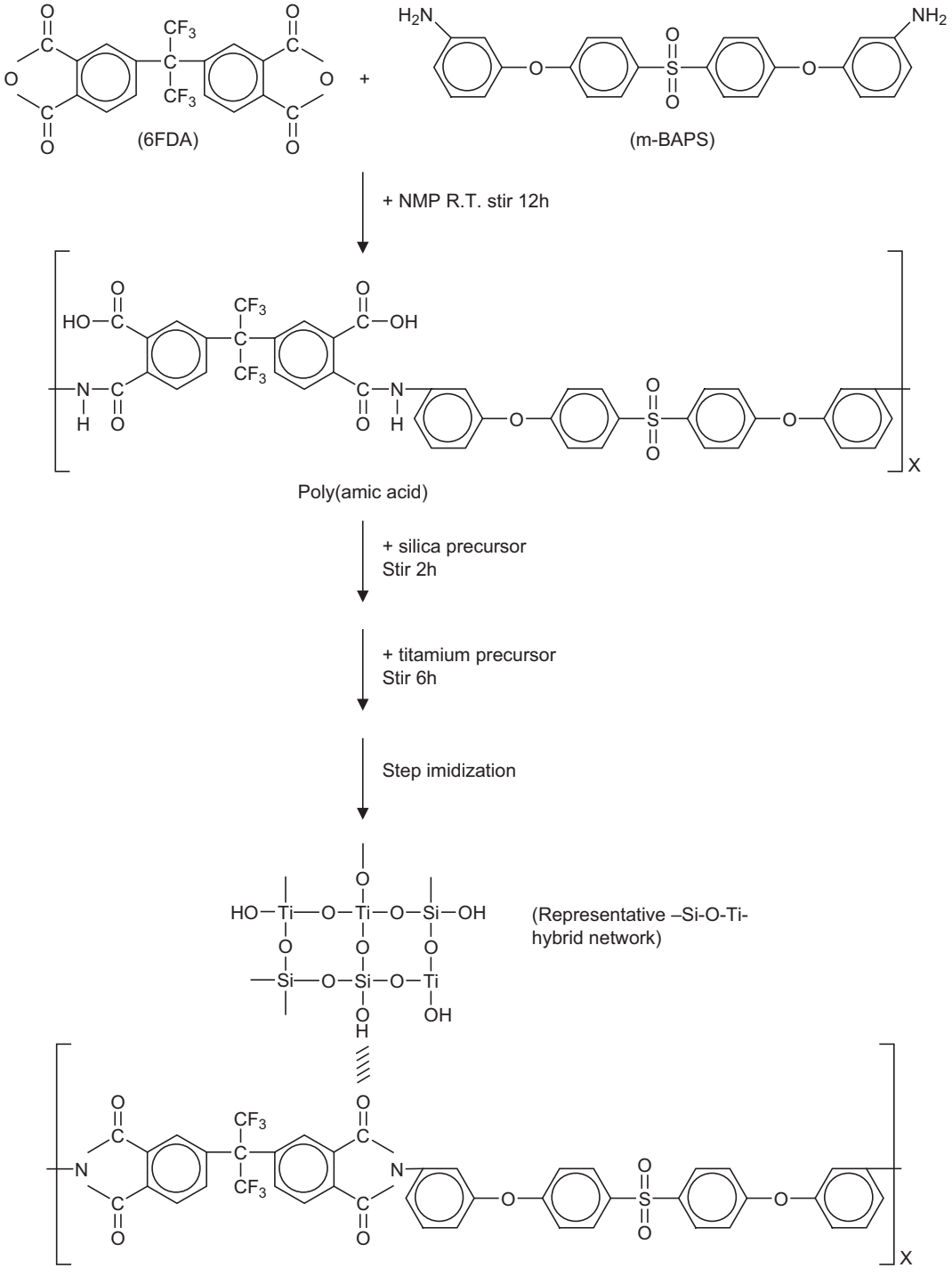

Scheme 1 Preparation of the PI/SiO2–TiO2 ternary hybrid nanocomposite. 6FDA, hexofluoropropane dianhydride; m-BAPS, bis [4-(3-aminophenoxy) phenyl sulfone; NMP, *N*-methyl-2-pyrrolidone; PI, polyimide.

It is worth noting that the surface roughness of neat PI could very well be caused by dehydration shrinkage during imidization. It was anticipated that, with the added inorganic hybrid particles, *R*a would increase because of the presence of immiscible inorganic particles (for example, *R*a for PI/S15–T2 was 4.99 nm in Table 1). However, Table 1 shows that the value of *R*a for PI/S15–T3.75 (0.68 nm), PI/S15–T7.5 (0.38 nm) and PI/S15–T15 (0.35 nm) was much smaller than that of the neat PI (1.02 nm). This shows that at appropriate inorganic particle size and content, the inherent shrinkage could be partially offset and the surface roughness could be reduced by the presence of inorganic particles. In this case, the particle size was <10 nm, and the inorganic content was SiO_2=15 wt% and $TiO_2 > 3.75$ wt%. This effect was likely due to the rigidity of the inorganic particles.

Thermal properties

The temperature of decomposition (T_d) provides information on the temperature range within which the material is stable. The temperature at which 5% weight loss occurred was taken as T_d. Figure 8 depicts the thermal-gravimetric analysis curves of the PI, PI/SiO_2, PI/TiO_2 and PI/SiO_2–TiO_2 hybrid nanocomposites. No weight loss was observed at temperatures below 100 °C, indicating that there was no residual water or ethanol in the composite films (Scheme 1).

As listed in Table 1, T_d of PI was 532 °C, which increased to 553 °C after the incorporation of 15 wt% silica. The T_d of the composite decreased to 482 °C after the incorporation of 15 wt% titanate. Table 1 shows that when the silica concentration is fixed at 15 wt% T_d decreases with increasing titanium content.

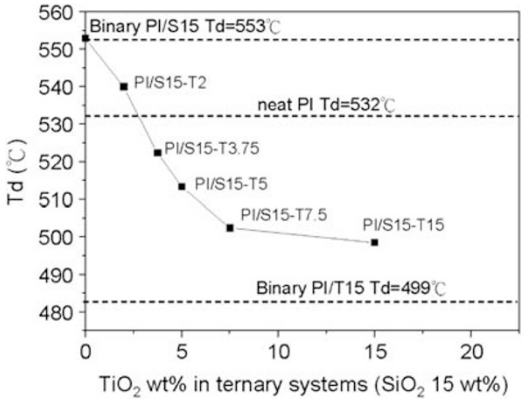

Figure 9 Comparison of T_d values for neat polyimide (PI), binary PI/S and PI/T, and ternary PI/SiO_2–TiO_2 systems.

In the study by Qiu *et al.*,[21] the T_d values of PI/ SiO_2–TiO_2 composites with 5–30 wt% total inorganic content and varied SiO_2/TiO_2 ratios (2:1, 1:1 and 1:2) were all higher than those of neat PI. Wang *et al.*[20] showed that the T_d values of the PI/ SiO_2–TiO_2 composites with 5–15 wt% total inorganic contents and varied TiO_2/SiO_2 ratios (9.0, 6.5 and 4.5) were all lower than those of neat PI. In this study, compared with the T_d of the neat PI, the T_d values of the ternary composites were higher at a titanium content lower than $\sim$2 wt%, and lower at titanium content greater than $\sim$3.75 wt%. Figure 9 compares the T_d values of the ternary hybrid composites with T_d values of the binary system (PI/S15 and PI/T15) and the neat PI (shown as dashed line in Figure 9). Perhaps because of the photo-catalytic character of TiO_2,[16,34–36] the thermal stability of PI/T15 decreased compared with neat PI, although PI/T15 was obtained as a nanocomposite.

The aforementioned differences in the trends of T_d with inorganic composition may have resulted from such factors as the manner in which titanium and silica are structurally arranged, the nature of the Si–O–Ti bond and the particle size. For various applications, T_d may be regarded as an important design variable. The aforementioned factors should be carefully investigated in designing such ternary composites in these applications and will be of significant interest in our future research.

UV–visible transmittance

The transmittance of the pure PI film was measured to be 97% at a wavelength of 500 nm, as shown in Figure 10. The film thickness was 5 μm, and the same thickness was used for both the binary and ternary systems. In the binary system, for PI/SiO_2 and PI/TiO_2, the transmittance dropped to 93 and 58%, respectively, at a SiO_2 or TiO_2 content of 15 wt% (Figure 10). However, in the ternary PI/SiO_2–TiO_2 system, fixing the SiO_2 content at 15 wt%, the transmittance decreased from 92 to 73% as the TiO_2 content was increased from 2 to 15 wt%.

The decrease in transmittance with increasing TiO_2 content may be attributed to two possible factors. One is the inherent photo-catalytic activity of nanosized TiO_2 particles on the polymer matrix, which is very likely to be oxidized by TiO_2 during imidization at high temperature. The other possibility may stem from the participation of acac,[16,37,38] which was used as a chelating agent for titanium cation in modulating the gelation rate of organic titanium (IV). It is quite likely that these two factors are both responsible for such variations in the optical properties and will be clarified in our future studies.

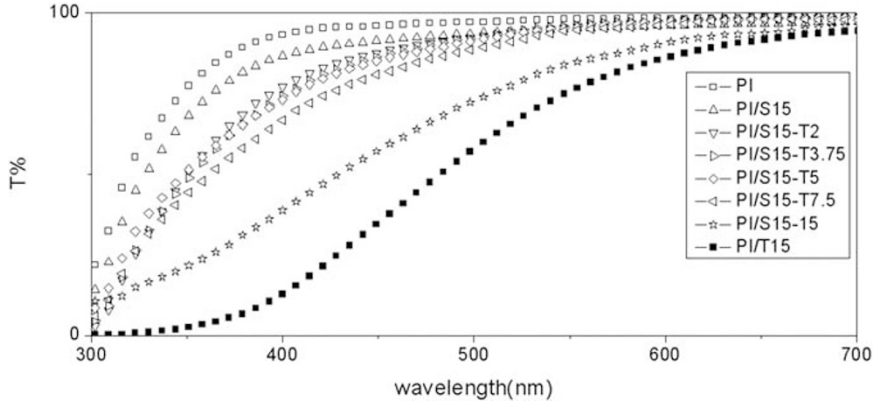

Figure 10 Optical transmittance of the nanocomposite films at various TiO_2 content (SiO_2 15 wt%). PI, polyimide.

CONCLUSION

In the PI/SiO_2–TiO_2 ternary hybrid nanocomposite materials studied here, SiO_2 complemented TiO_2 in a manner such that SiO_2 enhanced the thermal properties and TiO_2 contributed to reducing particle size. TiO_2 was shown to reduce the thermal stability of the material in the binary system (PI/TiO_2). Such a complementing effect was manifested by the formation of Si–O–Ti bonds according to the spectral data presented in this report. The chelating agent used in the sol-gel process might have contributed to controlling the fast gelling rate of TiO_2, allowing more opportunities for the formation of Si–O–Ti bonds. X-ray spectra also showed that the amount of TiO_2 in direct contact with the PI matrix was reduced; therefore, the impact of titanium's autocatalytic activity on the PI matrix was significantly reduced by SiO_2. The main contribution of the incorporated SiO_2 is to neutralize such hazardous catalytic destruction of TiO_2 on the polymer matrix that would otherwise lead to an autocatalytic breakdown of the polymer molecules.

1 Hu, X. & Zhao, X. Effects of annealing (solid and melt) on the time evolution of polymorphic structure of PA6/silicate nanocomposites. *Polymer* **45,** 3819–3825 (2004).
2 Kawasumi, M., Hasegawa, N., Kato, M., Usuki, A. & Okada, A. Preparation and mechanical properties of polypropylene-clay hybrids. *Macromolecules* **30,** 6333–6338 (1997).
3 LeBaron, P. C., Wang, Z. & Pinnavaia, T. J. Polymer-layered silicate nanocomposites: an overview. *Appl. Clay Sci.* **15,** 11–29 (1999).
4 Jiang, L., Wang, W., Wei, X., Wu, D. & Jin, R. Effects of water on the preparation, morphology, and properties of polyimide/silica nanocomposite films prepared by sol–gel process. *J. Appl. Polym. Sci.* **104,** 1579–1586 (2007).
5 Yang, C. P., Su, Y. Y. & Hsiao, S. H. Synthesis and properties of low-color polyimide/silica hybrid films. *J. Appl. Polym. Sci.* **104,** 4046–4052 (2007).
6 Park, H. B., Kim, J. H., Kim, J. K. & Lee, Y. M. Morphology of a poly(imide siloxane) segmented copolymer/silica hybrid composite. *Macromol. Rapid Comm.* **23,** 544–550 (2002).
7 Qiu, F., Zhou, Y., Liu, J. & Zhang, X. Preparation, morphological and thermal stability of polyimide/silica hybrid material containing dye NBDPA. *Dyes Pigments* **71,** 37–42 (2006).
8 Qin, J., Zhao, H., Liu, X., Zhang, X. & Gu, Y. Double phase separation in preparing polyimide/silica hybrid films by sol-gel method. *Polymer* **48,** 3379–3383 (2007).
9 Wang, L., Tian, Y., Ding, H. & Li, J. Microstructure and properties of organosoluble polyimide/silica hybrid films. *Eur. Polym. J.* **42,** 2921–2930 (2006).
10 Zhang, Y. H., Li, Y., Fu, S. Y., Xin, W., Daoud, A. & Li, L. F. Synthesis and cryogenic properties of polyimide–silica hybrid films by sol–gel process. *Polymer* **46,** 8373–8378 (2005).
11 Chiang,, P. C., Whang,, W. T., Tsai, S. & Wu, M. H. C. Physical and mechanical properties of polyimide/titania hybrid films. *Thin Solid Films* **447–448,** 359–364 (2004).
12 Kong, Y., Du, H., Yang, J., Shi, D., Wang, Y., Zhang, W. & Xin, Y. Study on polyimide/TiO_2 nanocomposite membranes for gas separation. *Desalination* **146,** 49–55 (2002).
13 Chang, C. M., Chang, C. L. & Chang, C. C. Synthesis and optical properties of soluble polyimide/titania hybrid thin films. *Macromol. Mater. Eng.* **291,** 1521–1528 (2006).
14 Chang, C. C. & Chen, W. C. High-refractive-index thin films prepared from aminoalkoxysilane-capped pyromellitic dianhydride–titania hybrid materials. *J. Polym. Sci. Part A Polym. Chem.* **39,** 3419–3427 (2001).
15 Tsai, M. H., Liu, S. J. & Chiang, P. C. Synthesis and characteristics of polyimide/titania nano hybrid films. *Thin Solid Films* **515,** 1126–1131 (2006).
16 Chiang, P. C. & Whang, W. T. The synthesis and morphology characteristic study of BAO-ODPA polyimide/TiO_2 nano hybrid films. *Polymer* **44,** 2249–2254 (2003).
17 Liu, L., Lu, Q., Yin, J., Qian, X., Wang, W., Zhu, Z. & Wang, Z. Photosensitive polyimide (PSPI) materials containing inorganic nanoparticles (I)PSPI/TiO2 hybrid materials by sol–gel process. *Mater. Chem. Phys.* **74,** 210–213 (2002).
18 Liaw, W. C. & Chen, K. P. Preparation and properties of poly(imide siloxane) segmented copolymer/silica hybrid nanocomposites. *J. Appl. Polym. Sci.* **105,** 809–820 (2007).
19 Liaw, W. C. & Chen, K. P. Preparation and characterization of poly(imide siloxane) (PIS)/titania(TiO_2) hybrid nanocomposites by sol-gel processes. *Eur. Polym. J.* **43,** 2265–2278 (2007).
20 Wang, H., Zhong, W., Xu, P. & Du, Q. Polyimide/silica/titania nanohybrids via a novel non-hydrolytic sol–gel route. *Compos. Part A* **36,** 909–914 (2005).
21 Qiu, W., Luo, Y., Chen, F., Duo, Y. & Tan, H. Morphology and size control of inorganic particles in polyimide hybrids by using SiO_2–TiO_2 mixed oxide. *Polymer* **44,** 5821–5826 (2003).
22 Tong, Y., Li, Y., Xie, F. & Ding, M. Short communication preparation and characteristics of polyimide-TiO_2 nanocomposite film. *Polym. Int.* **49,** 1543–1547 (2000).
23 Chen, H. J., Wang, L. & Chiu, W. Y. Chelation and solvent effect on the preparation of titania colloids. *Mater. Chem. Phys.* **101,** 12–19 (2007).
24 Fu, Y., Jin, Z., Ni, Y., Du, H. & Wang, T. Microstructure, optical and optoelectrical properties of mesoporous nc-TiO_2 films by hydrolysis-limited sol-gel process with different inhibitors. *Thin Solid Films* **517,** 5634–5640 (2009).
25 Ando, S. Optical properties of fluorinated polyimides and their applications to optical components and waveguide circuits. *J. Photopolym. Sci. Tec.* **17,** 219–232 (2004).
26 Liaw, D. J. & Liaw, B. Y. Synthesis and properties of polyimides derived from 3,3′,5,5′-tetramethyl-bis(4-(4-aminophenoxy)phenyl¡sulfone. *Eur. Polym. J.* **33,** 1423–1431 (1997).
27 Pramanik, N. C., Seok, S. I. & Ahn, B. Y. Wet-chemical synthesis of crystalline $BaTiO_3$ from stable chelated titanium complex: formation mechanism and dispersibility in organic solvents. *J. Colloid Interf. Sci.* **300,** 569–576 (2006).
28 Wu, K. H., Chang, T. C., Wang, Y. T. & Chiu, Y. S. Organic-inorganic hybrid materials. i. characterization and degradation of poly(imide–silica) hybrids. *J. Polym. Sci. Part A Polym. Chem.* **37,** 2275 (1999).
29 Essa, I. M., Essa, A. A. & Makadsi, M. N. IR, ESCA and Auger analysis of thermally hydrogenated a-Si:H thin films. *Sol. Energ. Mat. Sol. C.* **39,** 19–25(1995).
30 Gan, S., Yang, P. & Yang, W. T. Interface-directed sol-gel: direct fabrication of the covalently attached ultraflat inorganic oxide pattern on functionalized plastics. *Sci. China Chem.* **53,** 173–182 (2010).
31 Wang, L., Tian, Y., Ding, H. & Li, J. Microstructure and properties of organosoluble polyimide/silica hybrid films. *Eur. Polym. J.* **42,** 2921–2930 (2006).
32 Feng, L., He, L., Ma, Y. & Wang, Y. Grafting poly(methyl methacrylate) onto silica nanoparticle surfaces via a facile esterification reaction. *Mater. Chem. Phys.* **116,** 158–163 (2009).
33 Georgiev, D. G., Baird, R. J., Newaz, G., Auner, G., Witte, R. & Herfurth, H. An XPS study of laser-fabricated polyimide/titanium interfaces. *Appl. Surf. Sci.* **236,** 71–76 (2004).
34 Sharma, S. D., Singh, D., Saini, K. K., Kant, C., Sharma, V., Jain, S. C. & Sharma, C. P. Sol–gel-derived super-hydrophilic nickel dopedTiO_2 film as active photo-catalyst. *Appl. Catal. A-Gen.* **314,** 40–46 (2006).
35 Wu, C. G., Chao, C. C. & Kuo, F. T. Enhancement of the photo catalytic performance of TiO_2 catalysts via transition metal modification. *Catal. Today* **97,** 103–112 (2004).
36 Awitora, K. O., Rafqah, S., Geranton, G., Sibaud, Y., Larson, P. R., Bokalawela, R. S. P., Jernigen, J. D. & Johnson, M. B. Photo-catalysis using titanium dioxide nanotube layers. *J. Photoch. Photobio. A* **199,** 250–254 (2008).
37 Que, W., Zhou, Y., Lam, Y. L., Chan, Y. C. & Kam, C. H. Optical and microstructural properties of sol-gel derived titania/organically modifed silane thin flms. *Thin Solid Films* **358,** 16–21 (2000).
38 Yoshida, M. & Prasad, P. N. Sol-gel-processed SiO_2/TiO_2/poly(vinylpyrrolidone) composite materials for optical waveguides. *Chem. Mater.* **8,** 235–241 (1996).